Proceedings of the
Annual Stability Conference
Structural Stability Research Council
St. Louis, Missouri, April 2-5, 2019

Stability of apex connections in cold-formed steel portal frames

Hannah B. Blum[1], Zhanjie Li[2]

Abstract

Cold-formed steel portal frames are popular structures in industrial and residential sectors, and are commonly used in rural areas for sheds, garages, and shelters. The connections are an integral part of the structure and should have adequate strength to transfer the internal forces between the framing members. The connection stiffness affects the overall frame internal force and moment distributions and deflections. A recent experimental investigation was conducted to determine apex connection strength and stiffness in cold-formed steel portal frames for various rafter channel depths and thicknesses subjected to an opening bending moment. It was found that all specimens failed by apex bracket web buckling. However, the characteristic behavior of the connection was affected by the ratio of the geometric stiffness of the rafter to bracket, and low ratios resulted in an early reduction of connection stiffness compared to connections with higher ratios. Additionally, nominally identical connections showed a variation in strength and connection deflection behavior. An advanced finite element model was created and compared with the experimental results. Modeling details required to accurately capture the instabilities on the connection are discussed, as well as future improvements and parametric studies to further understand the behavior of the apex connection.

1. Introduction

Portal frames are commonly used to provide large open spaces for industrial, farming, and residential purposes. They are mostly used as sheds, garages, and shelters, and are especially common in rural areas. Traditionally, portal frames are composed of hot-rolled steel sections, but long-span cold-formed steel portal frames are becoming increasingly popular structures. There are several benefits to using cold-formed steel sections, including reduced material, fabrication, transport, and construction costs, and a higher strength to weight ratio compared to hot-rolled steel. However, cold-formed steel structures cannot be constructed or analyzed using the same methods as hot-rolled steel structures as they are prone to local and distortional buckling, as well as global buckling, and the interaction of these buckling modes. Additionally, as the elements are thin, connections in cold-formed steel portal frames are usually formed through mechanical fastening or interlock, such as bolting of plates or brackets in between the channel sections, as opposed to welded connections in their hot-rolled counterparts. These cold-formed steel

[1] Assistant Professor, Department of Civil & Environmental Engineering, University of Wisconsin-Madison, Hannah.blum@wisc.edu
[2] Assistant Professor, Department of Engineering, SUNY Polytechnic Institute, Utica, NY, Zhanjie.li@sunyit.edu

connections are found to be semi-rigid (Yu et al. 2005). The internal actions and deflections of portal frames are affected by the connection stiffness and behavior, and therefore it is important to correctly quantify connection strength and stiffness to accurately determine portal frame behavior. The apex connection of a portal frame is where the two rafter sides are connected together and is sometimes referred to as the ridge of the portal frame.

Finite element modeling has been previously used for parametric studies of portal frames to determine the effects of various components on the frame. A parametric study was used to determine the effect of knee braces with pinned or rigid connections at the joints to frames with rigid joints only (Wrzesien & Lim 2008), and to study the effects of the size of the connection brackets (Lim & Nethercot 2002). A parametric study was completed to determine if frames designed based on a rigid and full strength joint assumptions were safe under gravity load (Jackson et al. 2012).

Finite element models were created of the apex connection of a cold-formed steel portal frame with back-to-back bolted channels for the rafters and back-to-back bolted lipped L-plates for the apex brackets to further study the behavior of this connection. Finite element models must include all necessary components to accurately capture correct behavior. This could include exact material properties if yielding and spread of yielding are crucial, or geometric imperfections if buckling behavior is prominent or if the structure is sensitive to initial imperfections. Modeling bolts and bolt-holes are important if bolt-hole elongation is present, as was determined in (Lim & Nethercot 2002), or could be simplified as rigid connectors if bolts are sufficiently tight and bolt-slip is not present. It was determined in (Blum & Rasmussen 2019) that contact did not need to be modeled in between back-to-back channels in cold-formed steel portal frames as the minimal mesh penetrations did not affect overall frame results due to the column buckling failure mode. However, this assumption could change depending on the structure and connection being modeled. Simplified models are easier to create and require less time to run. Therefore, it is important to determine which factors must be included in a finite element model and which simplifications can be made to produce accurate results.

2. Background

A series of twelve tests on the apex connections of cold-formed steel portal frames has been conducted (Peng et al. 2018). The rafters consisted of back-to-back lipped channels bolted together through the webs, and the apex brackets consisted of back-to-back lipped L-brackets bolted through the webs. Various channel sizes and thickness were tested, including section depths of 203 mm with a thickness of either 1.5, 1.9, or 2.4 mm, and section depths of 152 mm with a thickness of 1.5, 1.9, or 2.4 mm. There were two apex bracket sizes: one for the 203 mm depth channels, and one for the 152 mm depth channels, both of which were 2.4 mm thick. The apex connection specimens were approximately 2 m long. The channel and apex brackets were bolted together with grade 8.8 M14 bolts for the C150 tests, and M16 bolts for the C200 tests. At other locations, the channels were bolted together with grade 4.6 M12 bolts with integrated washers. The channels and the apex brackets were fabricated using G450 steel, which indicates a nominal minimum yield stress of 450 MPa. Coupon tests from the channels and brackets were conducted according to the Australian Standard (AS 1391 2007) and it was found that the material had an average Young's Modulus of 206 GPa and an average 0.2% proof stress of 508 MPa. Further details are given elsewhere (Peng et al. 2018). All specimens failed by buckling of

the apex bracket. However, the overall stiffness behavior of the connection was affected by the ratio of the geometric stiffness of the rafter to bracket. Specimens with low ratios showed an early reduction in overall connection stiffness than specimens with higher ratios. Additionally, nominally identical connections showed a variation in ultimate load and deflections. To further investigate this behavior finite element models were created of the test specimens and compared with experimental results. The main details of the test specimens are given below.

Symmetric point loads were applied on the rafters to produce a constant bending moment in the apex connection. In the apex region of a portal frame with applied gravity loads, the apex is under a constant bending moment. Vertical load was applied by a hydraulic jack which was displacement controlled at a rate of 0.2mm/min. Downwards load was applied to cause the connection to open, as would occur due to gravity loads. Lateral restraints, consisting of two turnbuckles each, were connected at four locations along the rafters at the locations where purlins would be connected in full frames. The rafter ends were supported by two half-rounds which were inclined to be perpendicular to the rafters. Rafter boots were bolted onto the rafter ends to increase the torsional rigidity of the specimen ends.

Four inclinometers were placed inside the apex bolt-group centers, one on each side of the connection both on the front and back channels, to measure the in-plane rotation of the connection. Inclinometers were attached on the rafter longitudinal center-lines. The two front inclinometers are shown in the blue circles in Fig. 1. The front and back inclinometer readings were averaged, and each side of the connection was considered a spring in series in order to calculate a total rotational spring for the center of the connection. Linear variable displacement transducers (LVDTs) were placed at the bracket center, both front and back, to measure global movements vertically, and are shown in the green circle in Fig. 1. Measurements were recorded from the attached measuring plates which were located at the bottom of the apex bracket. Three LVDTs were positioned at the apex bracket, two on the front face near the rafter, and one on the back face on the center of the bracket, to measure out-of-plane displacements. The front two LVDTs are shown in the yellow circle in Fig. 1. The bending moment in the apex was calculated from the applied load using statics.

As load was applied causing an opening of the apex connection, the specimen deflected downwards. Eventually, the apex bracket began to buckle in the web, where one side deflected forwards and the other side deflected backwards by a few millimeters. A failed specimen is shown in Fig. 4. Load application continued after reaching the ultimate load to capture post-peak behavior. The apex bracket web out-of-plane displacements increased after reading peak load. This produced an eccentricity in the load path of the two rafters, which resulted in a significant reduction in the post-peak connection rotational stiffness. All specimens had similar failure modes. Out-of-plane rotations were measured during the test with the vertical LVDTs, as shown in Fig. 1. At peak load, the rotations were small but increased during post-peak loading. Full results of the out-of-plane rotations and displacements for each test are given elsewhere (Peng 2017; Bendit 2017).

As the connection opened, the top of apex bracket web was under compression. Failure occurred in the apex bracket, as there was no top flange to restrain the top edge of the web from buckling. Additionally, the center of the apex bracket is a weak point in the connection, as the rafters were

not connected at this location, thus solely the apex brackets were resisting the applied loads. After removal of the load the specimens were disassembled. Permanent deformations remained in the apex bracket web, as shown in Fig. 4. No plastic deformation was evident on the rafters, and no bolt-hole elongation was evident in either the rafters or apex brackets.

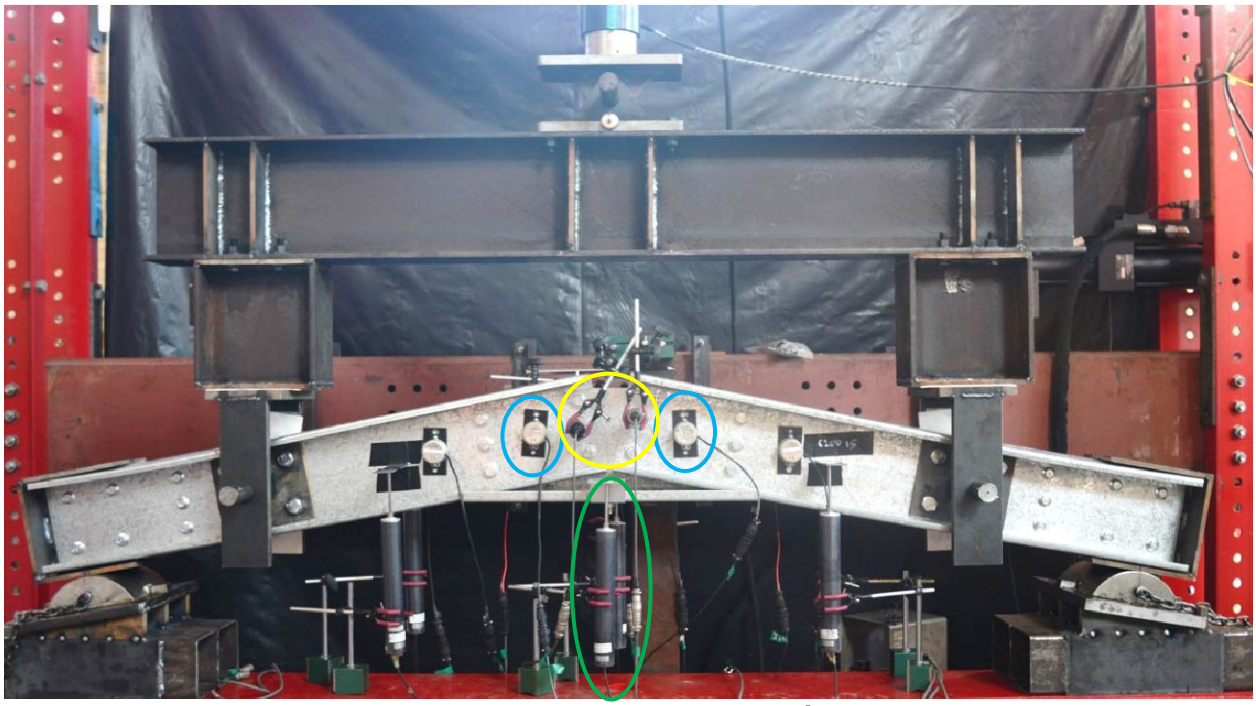

Figure 1: Apex connection experimental setup

The bending moment vs. rotation curves for the apex connection are shown in Fig. 2. As the thickness of the connected rafters increases, the initial in-plane rotational stiffness increases. However, this initial linear region is significantly smaller for C150-24 specimens. In Fig. 2(b) it is shown that the C150-24 curves are almost bi-linear, whereas the C150-15 and C150-19 specimens (Fig. 2(a)) do not show this behavior. In Table 1, the ratio of $I_{x,bracket}$ to $I_{x,rafter}$ is presented. The lowest ratio is 0.79 for the C150-24 specimens. In this case the rafter sections are significantly flexurally stiffer than the apex brackets, and this creates a local weak area in the apex connection. It is hypothesized that as loading increases, it becomes easier for the apex bracket to deflect rather than bending in the rafters or in the combined system, which results in an earlier loss of stiffness in the connection compared to the specimens with higher $I_{x,bracket}$ to $I_{x,rafter}$ ratios. It could be argued that the C200-24 specimens (Fig. 2(d)) slightly show a similar trend to the C150-24 specimens, although the change in slope is much less pronounced and occurs at a higher bending moment. Although the C150 connection specimens with thicker rafters (2.4 mm) are stronger than those having thinner rafters (1.9 mm and 1.5 mm), there is an earlier loss of stiffness in the connection. As apex connection stiffness affects the overall deflection in the frame, is it crucial to study this connection.

Finite element models of the connections tested in (Peng et al. 2018) were created and compared against the experimental results. Models were studied to determine which modeling parameters are crucial to obtain correct output, and which modeling parameters are not necessary. The effect

of imperfections on the test rig setup was included to aid in convergence of the models and to include possible effects in a test rig.

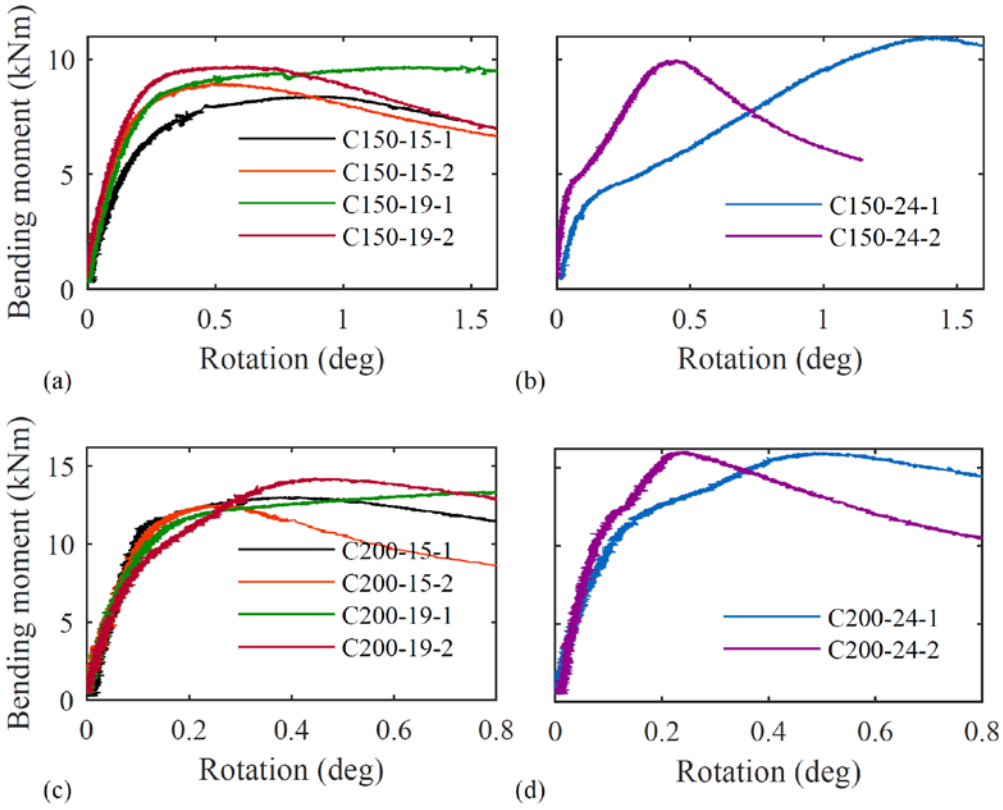

Figure 2: Bending moment vs. rotation at the apex connection

Table 1: Geometric stiffness ratio of bracket to rafter for each connection size

Connection	$I_{x,bracket} / I_{x,rafter}$
C150-15	1.25
C150-19	1.00
C150-24	0.79
C200-15	1.39
C200-19	1.09
C200-24	0.86

3. Model details

Advanced shell finite element models were created in ABAQUS (ABAQUS 2014a) of the apex connection tests described previously. Measured dimensions and thicknesses of the channel sections and apex brackets were used in the models. Nominal dimensions are given in Table 2, and measured dimensions are provided in (Peng 2017; Bendit 2017) and complete dimensions of the apex brackets are given in (Peng et al. 2018). The model was first created in SolidWorks, then the geometry was imported into ABAQUS. The channel sections and apex brackets were modeled with 4-node doubly curved shell elements with linear interpolation, reduced integration and hourglass control (S4R elements). Bolts in the connections were modeled using multi-point-

based coupling constraints (MPC beam). This uses distributed coupling constraints to connect the faces of elements through either couplings or connectors (ABAQUS 2014b). First, an attachment point was defined at the location of a bolt, which was projected though the specified numbers of layers in a specified direction to connect the members at the location of the bolt. The physical radius of the connector was specified in the fastener definition and was equal to the radius of the bolt. A rigid beam multi point constraint was chosen to model the bolts assuming the bolts were sufficiently tight and there was no bolt slip. As bolts were tightened using the snug tight plus half a turn method, and no visible bolt-hole elongation or bolt-slip was visible during the experiments, this assumption is valid. Structural distributing was chosen as the fastener formulation, which couples the displacements and rotations of the fastening points to the average displacement and rotation of the nodes. All bolts were modeled in this manner. Contact and friction were modeled between the webs of back-to-back apex brackets and channel sections. Hard contact was defined in the normal direction, and a coefficient of friction of 0.5 in the tangent direction. The material properties of the channels and apex connection brackets were modeled as an elastic perfectly curve with a Young's Modulus of 206 GPa and a 0.2% proof stress of 508 MPa, as measured during tensile coupon tests (Peng 2017; Bendit 2017). The stress and strain was converted to true stress and true strain and inputted into the material property definitions in ABAQUS (ABAQUS 2014a).

Table 2: Nominal dimensions and thickness of connected members in the apex connection tests

Test #	Channel	Channel dimensions (mm)		Apex bracket	
		web × flange × lip	*t* (mm)	Size	*t* (mm)
1, 2	C200-15	203 × 76 × 15.5	1.5	C200	2.4
3, 4	C200-19	203 × 76 × 19.0	1.9	C200	2.4
5, 6	C200-24	203 × 76 × 21.0	2.4	C200	2.4
7, 8	C150-15	152 × 64 × 15.5	1.5	C150	2.4
9, 10	C150-19	152 × 64 × 16.5	1.9	C150	2.4
11, 12	C150-24	152 × 64 × 18.5	2.4	C150	2.4

In the experimental setup, the ends of the rafters had rafter boots to increase the torsional rigidity of the channels, and was placed on top of half-rounds to support the connection vertically but to allow for horizonal movements as the connection opened up under load. To represent these effects, the ends of the rafters are restrained against twist along the longitudinal axis of the rafter by analytically tying all the nodes at the ends and restraining the corresponding twist degree of freedom. To simulate the roller support, the rafter ends are restrained from lateral displacements but allow longitudinal displacement. In the experiment, lateral restraints (in the form of turnbuckles connected to a support frame) were provided to the purlin brackets. Therefore, in the model, the nodes at the locations of the purlin brackets were restrained in the out-of-plane direction to represent these supports. To prevent rigid body motion of the connection, several nodes in the center of the apex bracket were restrained from moving horizontally. In the experiments, loads were applied through the loading pin which acted though the centroid of the rafter channel sections. In the models, a rigid body was created by tying all the nodes at the location of the loading pin hole to the center of the hole and then the prescribed displacement was applied at the center reference node. This permitted the displacement-controlled loading method. To consider the effects of the imperfections resulting from offsets in the testing rig, an initial displacement was introduced on the loading application reference node, which essentially modeled potential offsets introduced when placing a specimen inside a testing rig. This also helped to promote convergence of the initial perfect model. The imperfections were equal and

opposite in sign, being -1 mm at the left-side loading plate and +1 mm at the right-side loading plate. This initial displacement step was analyzed first using the static, general method before vertical load was applied.

A geometric and material nonlinear static analysis was completed. Due to the convergence issue of the contact modeling, the analysis was a general static analysis with stabilization by displacement control. Residual stresses were not modeled as the through-thickness residual stress is accounted for in the finite element models through the measured stress-strain curve determined from coupon tests, and membrane residual stresses are small relative to the yield stress in cold-formed steel sections (Moen et al. 2008). The mesh size was approximately 10 mm for all members in the connection. The layout of the finite element model with rafter channels and apex brackets for a C150 specimen is shown in Fig. 3.

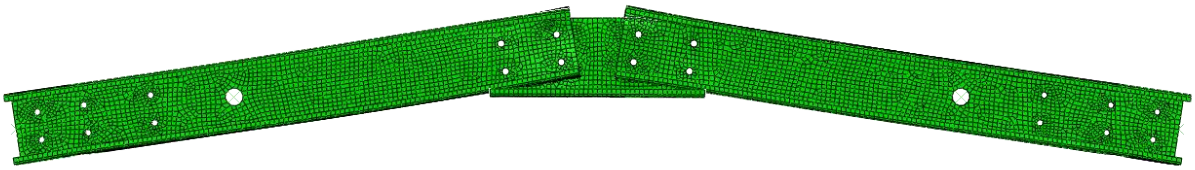

Figure 3: FEM of a C150 apex connection

4. Results

Finite element models were run for each of the various size apex connections. The ultimate moment capacities of the connections are shown in Table 3 for both the experiments and the finite element results. The finite element models were able to capture the failure mode, which was buckling of the apex bracket web, where each side of the bracket moved in opposite directions out of the plane of the connection. There was no buckling of the rafter channel sections, which agrees with the experiments. The deformed shape of the connection is shown in Fig. 4 for both the experiment and finite element model, and the permanent deformation of the apex brackets is shown in Fig. 5 for both the experiment and finite element model.

Table 3: Ultimate moment capacity of apex connections

Test	Ultimate moment (kN-m)		% difference
	Experiment	FE results	
C200-15-1	13.1	11.6	-11.5
C200-15-2	12.5		-7.2
C200-19-1	13.4	14.9	11.2
C200-19-2	14.2		4.93
C200-24-1	16.0	17.0	6.25
C200-24-2	16.0		6.25
C150-15-1	8.39	8.16	-2.74
C150-15-2	8.99		-9.23
C150-19-1	9.71	8.89	-8.44
C150-19-1	9.71		-8.44
C150-24-1	11.0	9.51	-13.5
C150-24-2	9.97		-4.61

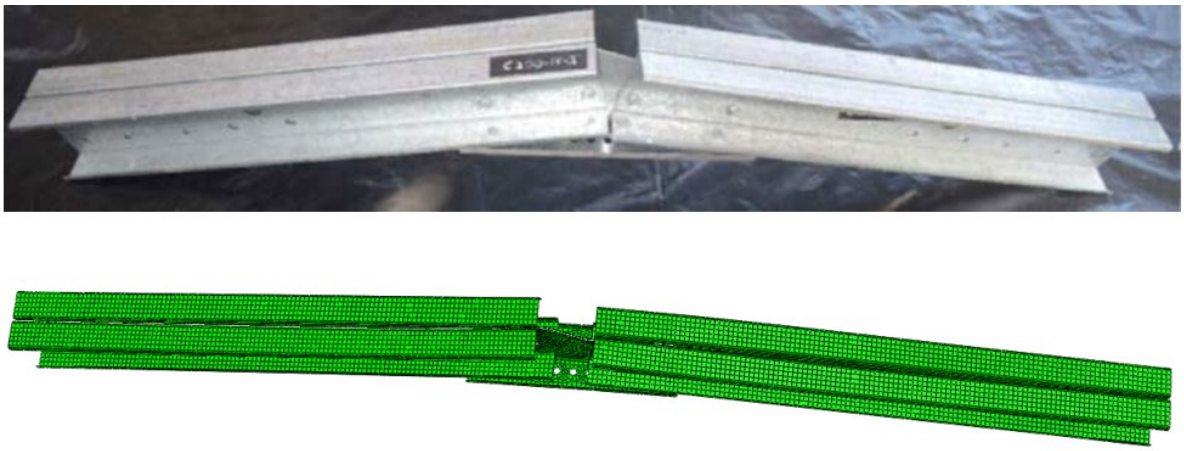

Figure 4: Failed apex connection specimen

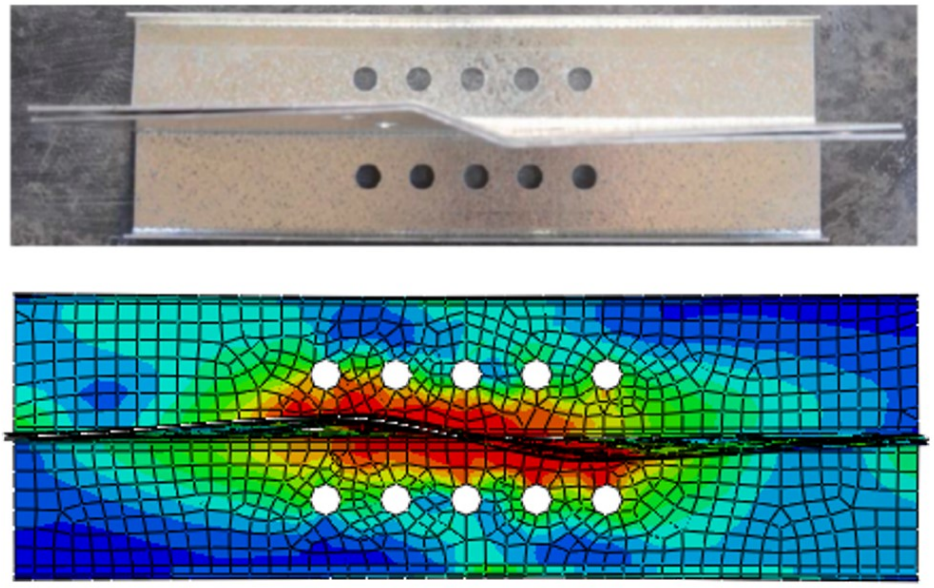

Figure 5: Bucked apex connection bracket (top view)

Bending moment versus rotation plots were created for all test specimens and their related finite element models, as this is the behavior of interest in the connection. Rotation values from the finite element models were taken at the location of the inclinometers inside the apex connections, as shown in the blue circles in Fig. 1. Plots for the C150-15, C150-19, and C150-24 connections are shown in Fig. 6, Fig. 7, and Fig. 8, respectively. The finite element model for the C150-15 connection matches well with the C150-15-2 test specimen. The C150-19 model underestimates the rotation of the connection during pre-ultimate load levels, as does the C150-24 model. Additionally, the C150-24 model does not show the distinct bi-linear behavior of the connection that was evident from the experiments.

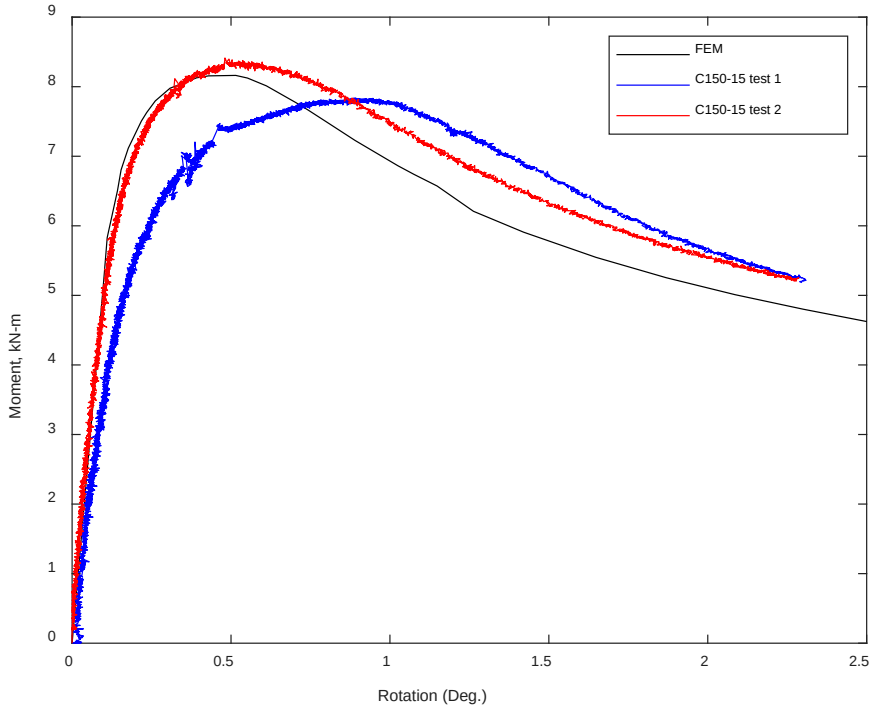

Figure 6: Moment vs. rotation for C150-15

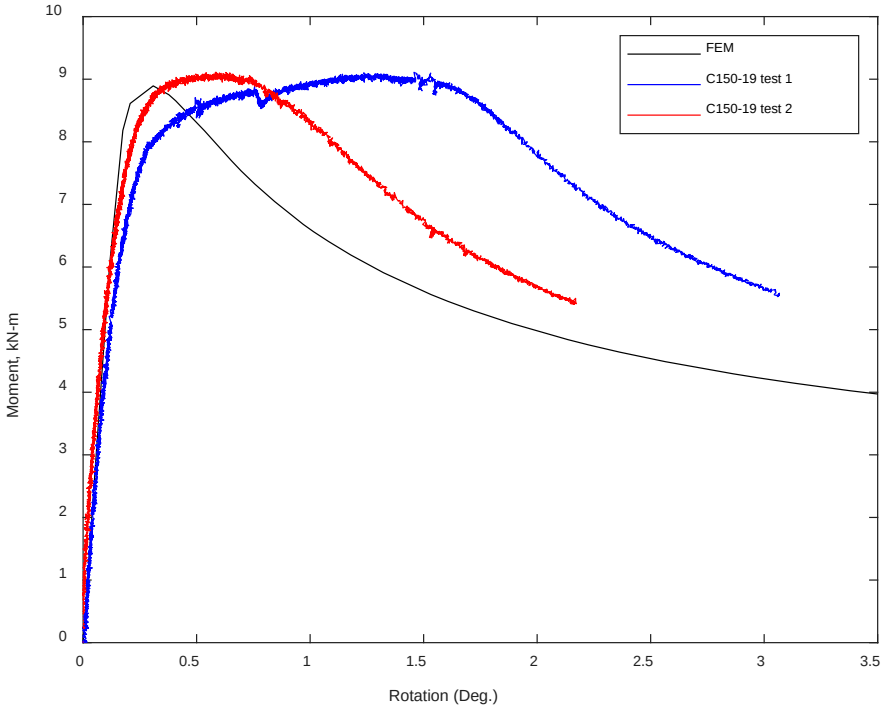

Figure 7: Moment vs. rotation for C150-19

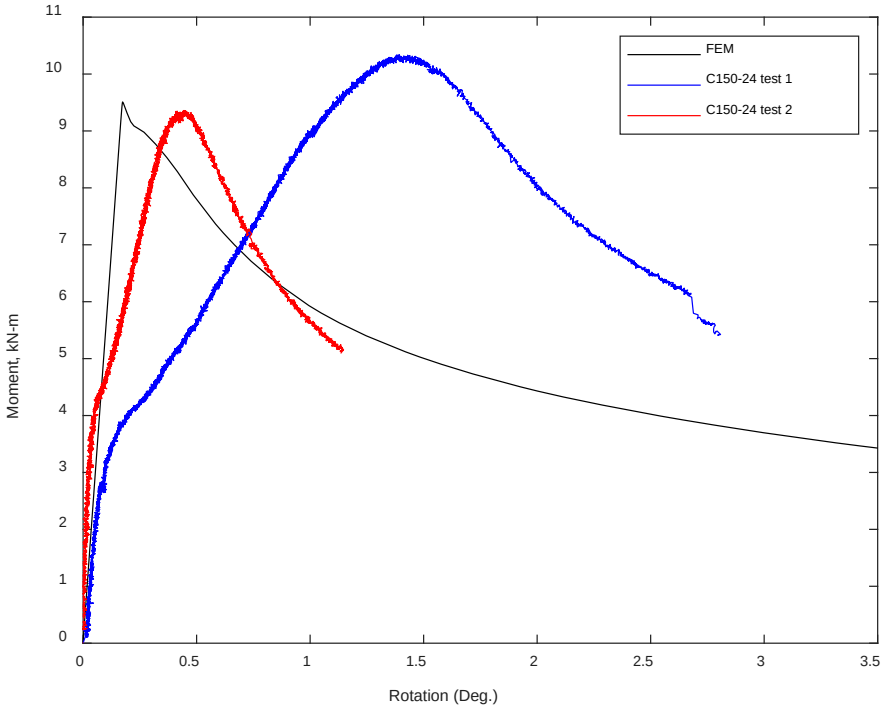

Figure 8: Moment vs. rotation for C150-24

Bending moment versus rotation plots are shown for the C200-15, C200-19, and C200-24 apex connections in Fig. 9, Fig. 10, and Fig. 11, respectively. The finite element model for the C200-15 connection matches well with the C200-15-1 test specimen. The C200-19 model underestimates the rotation of the connection during pre-ultimate load levels, as does the C200-24 model. Additionally, the C200-24 model does not show the bi-linear behavior of the connection that was can be seen from the experimental results. The C200-19 and C200-24 finite element models are the only models which overestimate the ultimate bending moment in the connection, all other models underestimate the ultimate bending moment between 3-13%, as shown in Table 3.

Overall, both the C150-15 and C200-15 finite element models best match the connection behavior measured in the experiments. Both connections have rafter channels with thickness of 1.5 mm. The connections with thicker rafter channels of 1.9 mm and 2.4 mm do not have finite element models that well match the connection behavior as measured in the experiments. Further analysis is required to refine the modeling method to improve the results of the connections with 1.9 mm and 2.4 mm thick rafter channel sections.

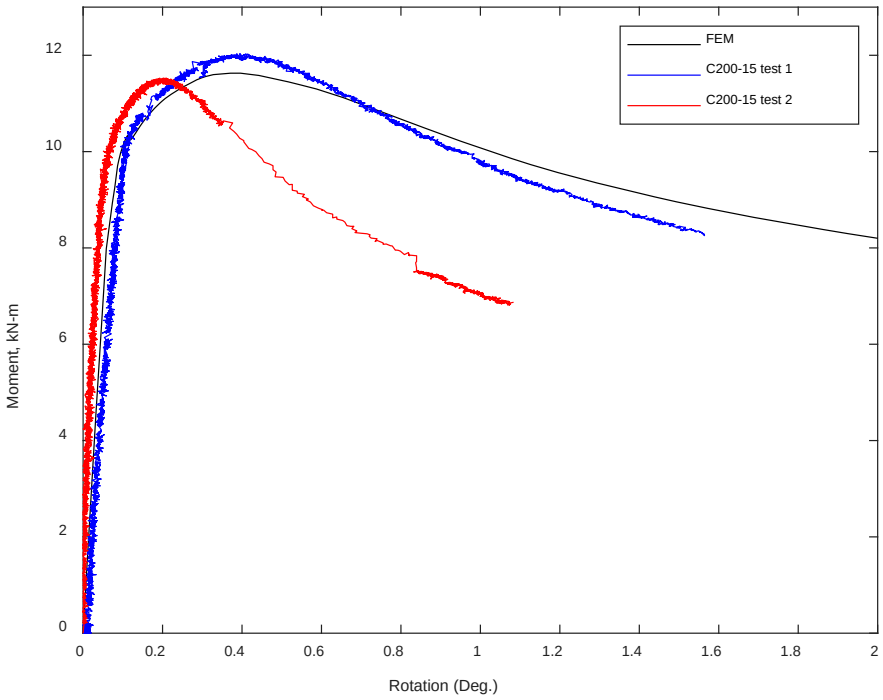

Figure 9: Moment vs. rotation for C200-15

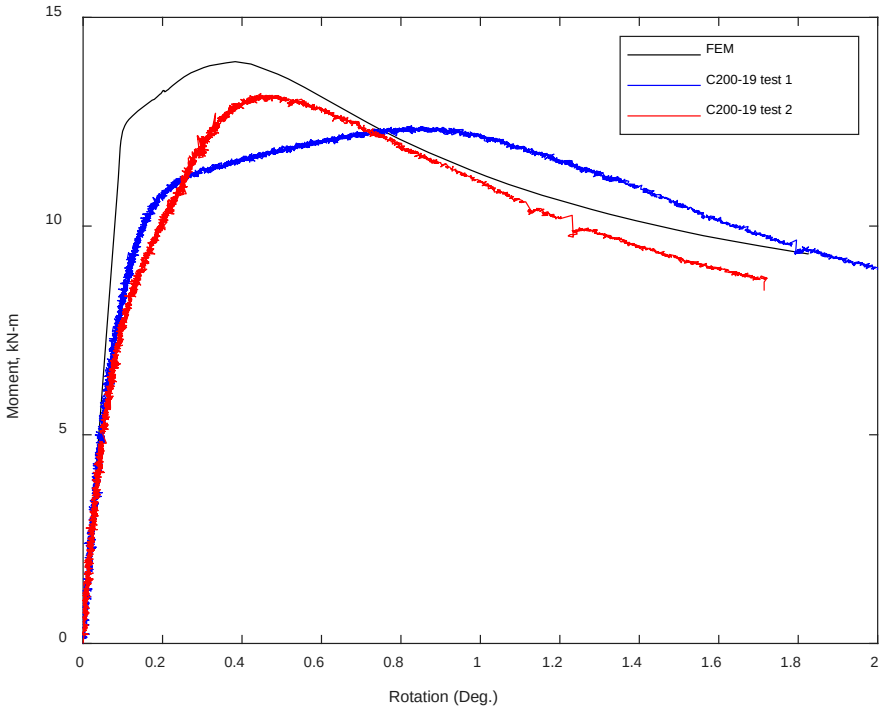

Figure 10: Moment vs. rotation for C200-19

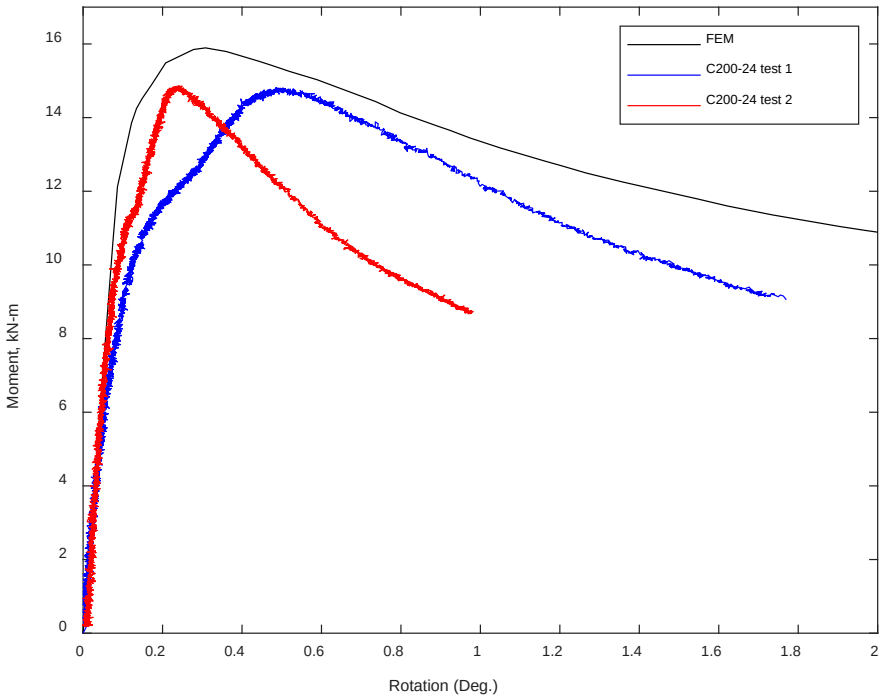

Figure 11: Moment vs. rotation for C200-24

5. Future work

Further model refinements are necessary to accurately capture the connection behavior for all channel rafter thicknesses, and to further reduce the percent difference in the ultimate bending moment between the finite element results and the experimental results. Next, the impact of imperfections on the apex bracket can be explored. This can be completed by imposing 1st order and 2nd order buckling mode imperfections on the initial geometry of the bracket, and then applying load to the connection. After the modeling method is verified, a parametric study can be completed to vary the ratio of $I_{x,bracket}$ to $I_{x,rafter}$ in order to determine at which ratio the connection behavior changes from linear to bi-linear before reaching ultimate capacity. Then, the verified model can be explored to determine potential apex bracket modifications to increase the strength of the connection by preventing buckling of the apex bracket web. Possibilities could include the addition of a top flange to the apex bracket.

6. Conclusions

Finite element models have been created of apex connection tests for various rafter channel thicknesses, depths, and apex bracket sizes. Bending moment versus apex rotation behavior of the finite element models were compared to the experimental tests of the apex connections. Overall, the models for both the C150-15 and C200-15 connections, which have 1.5 mm thick rafter channels, compared well with the experiments. The finite element models for the apex connections with 1.9 mm and 2.4 mm thick rafter channels underestimated the rotation behavior, and the finite element models for the 2.4 mm thick rafter channels did not capture the bi-linear behavior of the moment-rotation relationship. Ultimate bending moment of the connections from

the finite element models varied between 3 to 13% different to that of the experiments. Further refinement of the modeling method is required to accurately capture behavior of all apex connections.

Acknowledgements
The authors would like to thank Zachary King, a senior civil engineering student at SUNY Poly for his contribution of the SolidWorks modeling of the connection.

References

ABAQUS, 2014a. ABAQUS / Standard Version 6.14.

ABAQUS, 2014b. *ABAQUS Documentation*, Providence, RI, USA: Dassault Systemes.

AS 1391, 2007. *Australian Standards 1391: Metallic Materials - Tensile Testing at Ambient Temperature*,

Bendit, J., 2017. *Experimental Investigation of Apex Connection Moment-Rotational Stiffness in Cold-Formed Steel Portal Frames*. The University of Sydney.

Blum, H.B. & Rasmussen, K.J.R., 2019. Experimental and numerical study of connection effects in long-span cold-formed steel double channel portal frames. *Journal of Constructional Steel Research*, 155, pp.316–330. Available at: https://doi.org/10.1016/j.jcsr.2018.11.013.

Jackson, C. et al., 2012. Effect of reduced joint strength and semi-rigid joints on cold-formed steel portal frames. In *Proceedings Sixth International Conference on Coupled Instabilities in Metal Structures*. pp. 287–294.

Lim, J.B.P. & Nethercot, D.A., 2002. F.E.-assisted design of the eaves bracket of a cold-formed steel portal frame. *Steel and Composite Structures*, 2(6), pp.411–428.

Moen, C.D., Igusa, T. & Schafer, B.W., 2008. Prediction of residual stresses and strains in cold-formed steel members. *Thin-Walled Structures*, 46(11), pp.1274–1289.

Peng, J., 2017. *Experimental Investigation of Apex Connection Stiffness in Cold-Formed Steel Portal Frames*. The University of Sydney.

Peng, J., Bendit, J. & Blum, H.B., 2018. Experimental study of apex connection stiffness and strength of cold-formed steel double channel portal frames. In *Proceedings Twentyfourth International Specialty Conference on Cold-Formed Steel Structures*.

Wrzesien, A.M. & Lim, J.B.P., 2008. Cold-formed steel portal frame joints : a review. In *Proceedings Nineteenth International Specialty Conference on Cold-Formed Steel Structures*. St. Louis, Missouri, pp. 591–606.

Yu, W.K., Chung, K.F. & Wong, M.F., 2005. Analysis of bolted moment connections in cold-formed steel beam-column sub-frames. *Journal of Constructional Steel Research*, 61(9), pp.1332–1352.